Environmental controls on coral skeletal $\delta^{13}C$ in the northern South China Sea

Wenfeng Deng,[1] Gangjian Wei,[1] Luhua Xie,[2] and Kefu Yu[3]

Received 22 April 2013; revised 6 September 2013; accepted 7 September 2013.

[1] In this paper, we investigate the relationship between seasonal climatic and environmental variables, and the skeletal $\delta^{13}C$ of modern and mid-Holocene *Porites lutea* corals from the southern coast of Hainan Island in the northern South China Sea. No significant correlations were observed between $\delta^{13}C$ in the modern coral and solar insolation or sea surface temperature. However, seasonal variability of $\delta^{13}C$ in the modern coral covaries with rainfall on Hainan Island. Furthermore, the seasonal variations of $\delta^{13}C$ in both the modern and mid-Holocene coral are synchronous with those of the coral $\Delta\delta^{18}O$, which is a proxy for seawater $\delta^{18}O$ and, in turn, largely controlled by local rainfall. These observations suggest that coral $\delta^{13}C$ variations are closely associated with rainfall in this region. Given that river runoff contains dissolved inorganic carbon (DIC) with a negative $\delta^{13}C$, we suggest that periods of high rainfall on Hainan Island deliver increased amounts of ^{13}C-depleted DIC to coastal seawater, resulting in an enhanced negative $\delta^{13}C$ in the corals. Our findings, together with previous studies, appear to demonstrate that in coastal environments, coral skeletal $\delta^{13}C$ levels are controlled mainly by terrestrial carbon input and are significantly influenced by terrestrial river runoff. Consequently, the geochemical interpretation of coral $\delta^{13}C$ records may differ between coastal areas and offshore areas or the open ocean.

Citation: Deng, W., G. Wei, L. Xie, and K. Yu (2013), Environmental controls on coral skeletal $\delta^{13}C$ in the northern South China Sea, *J. Geophys. Res. Biogeosci.*, *118*, doi:10.1002/jgrg.20116.

1. Introduction

[2] Reef corals are widely used as archives of environmental and climatic change in tropical oceans. Stable oxygen isotopes ($\delta^{18}O$) preserved in coral skeletons are routinely used as a paleoclimatic proxy, and coupled with the Sr/Ca-derived sea surface temperature (SST) proxy, seawater $\delta^{18}O$ profiles can be used to investigate changes in local rainfall or evaporation [*Gagan et al.*, 1998; *Hendy et al.*, 2002; *McCulloch et al.*, 2003]. The use of coral $\delta^{13}C$ as a proxy for environmental and climatic change is, however, still a matter of debate [e.g., *Fairbanks and Dodge*, 1979; *Swart*, 1983; *McConnaughey*, 1989, 2003; *Swart et al.*, 1996a, 1996c; *McConnaughey et al.*, 1997; *Grottoli*, 2002; *Moyer and Grottoli*, 2011; *Allison and Finch*, 2012]. The response of coral skeletal $\delta^{13}C$ to changes in climatic and environmental variables is ambiguous because many factors, including carbon source, metabolic effects, and other environmental variables, are thought to influence coral skeletal $\delta^{13}C$ [e.g., *Swart*, 1983; *McConnaughey*, 1989; *Swart et al.*, 1996b; *McConnaughey et al.*, 1997; *Omata et al.*, 2008]. At the cellular scale, carbon precipitated in coral skeletons originates directly from dissolved inorganic carbon (DIC) in the extracellular-calcifying fluid (ECF), which forms an interior pool beneath the calicoblastic layer of coral polyps where calcification takes place [*Gattuso et al.*, 1999]. Inorganic carbon derived from metabolic respiration inside the coral polyps and external seawater may both contribute to the carbon in the ECF used for calcification, although the relative contributions from these two sources remain unknown [*Furla et al.*, 2000; *Al-Horani et al.*, 2003; *McConnaughey*, 2003]. Therefore, any biological or environmental factor that might influence $\delta^{13}C$ in these two sources of inorganic carbon input to the ECF may also affect $\delta^{13}C$ variations recorded in the coral skeleton.

[3] Numerous studies have attempted to address the causes of $\delta^{13}C$ variations in coral. One prevailing hypothesis is that increasing the rate of endosymbiotic zooxanthellae photosynthesis may induce an increase in skeletal $\delta^{13}C$ [*Swart et al.*, 1996b; *McConnaughey et al.*, 1997]. Consequently, many of these previous studies have focused on the climatic and environmental variables that influence the photosynthesis rate of zooxanthellae, such as light availability (cloud cover) and

[1]State Key Laboratory of Isotope Geochemistry, Guangzhou Institute of Geochemistry, Chinese Academy of Sciences, Guangzhou, China.
[2]Key Laboratory of Marginal Sea Geology, Guangzhou Institute of Geochemistry, Chinese Academy of Sciences, Guangzhou, China.
[3]Key Laboratory of Marginal Sea Geology, South China Sea Institute of Oceanology, Chinese Academy of Sciences, Guangzhou, China.

Corresponding author: W. Deng, State Key Laboratory of Isotope Geochemistry, Guangzhou Institute of Geochemistry, Chinese Academy of Sciences, 511 Kehua Street, Guangzhou, Guangdong 510640, China. (wfdeng@gig.ac.cn)

G. Wei, State Key Laboratory of Isotope Geochemistry, Guangzhou Institute of Geochemistry, Chinese Academy of Sciences, 511 Kehua Street, Guangzhou, Guangdong 510640, China. (gjwei@gig.ac.cn)

2169-8953/13/10.1002/jgrg.20116

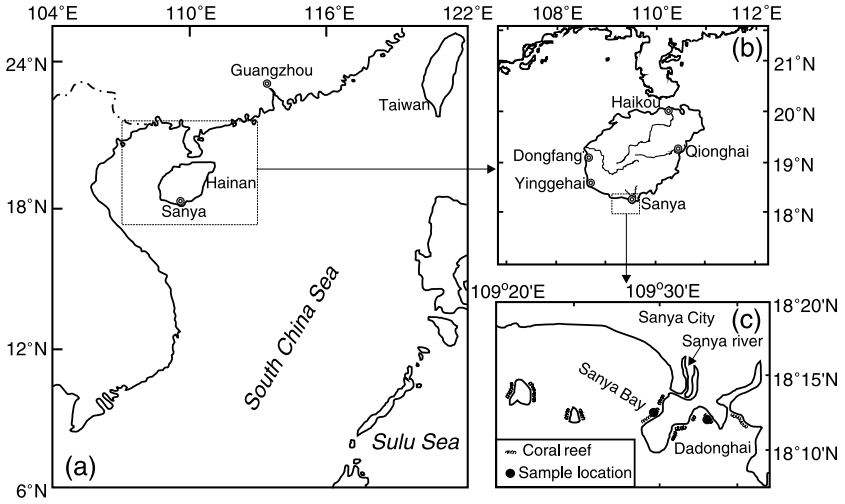

Figure 1. Location map of study site in the SCS showing (a) the northern SCS, (b) the Hainan Island, and (c) the Sanya coral reef and sample locations of the corals analyzed in this study. The modern coral was collected in Sanya Bay and the mid-Holocene coral in Dadonghai.

water depth [*Land et al*., 1975; *Weber et al*., 1976; *Fairbanks and Dodge*, 1979; *Swart et al*., 1996b; *Grottoli and Wellington*, 1999; *Heikoop et al*., 2000; *Grottoli*, 2002; *Maier et al*., 2003; *Rosenfeld et al*., 2003]. In addition, a wide range of other factors, such as kinetic isotope fractionation [*McConnaughey*, 1989], the $\delta^{13}C$ of DIC in seawater [*Swart et al*., 1996b; *Watanabe et al*., 2002; *Moyer and Grottoli*, 2011], the $\delta^{13}C$ of coral tissue and symbiotic zooxanthellae [*Swart et al*., 2005], feeding [*Grottoli*, 2002; *Reynaud et al*., 2002], spawning [*Gagan et al*., 1994, 1996], bleaching [*Porter et al*., 1989; *Leder et al*., 1991; *Allison et al*., 1996], and anthropogenic effects [*Swart et al*., 1996c, 2010; *Dassié et al*., 2013] have all been suggested as influences on coral skeletal $\delta^{13}C$.

[4] Amongst these potential factors, the effect of changes in $\delta^{13}C$ in seawater DIC on the $\delta^{13}C$ of coral skeletons has received less detailed attention than other factors. Due to the lack of continuous field observations, variations in seawater DIC $\delta^{13}C$ in most coral reefs are poorly constrained. Some studies have even assumed a constant $\delta^{13}C$ value of seawater DIC when considering the response of coral $\delta^{13}C$ to environmental variables [*Allison et al*., 1996; *Boiseau et al*., 1998]. However, natural variations in seawater $\delta^{13}C$ around many coral reefs cannot be neglected, particularly in some fringing reefs where the influence from river runoff can be significant [*Furnas*, 2003; *McCulloch et al*., 2003; *Fabricius*, 2005]. Input of river water with relatively depleted $\delta^{13}C$ levels (typically 0‰ to −26‰) [*Quay et al*., 1992; *Yang et al*., 1996; *Atekwana and Krishnamurthy*, 1998; *Palmer et al*., 2001] may significantly change the $\delta^{13}C$ (typically 1‰ to 3‰) of DIC in seawater [*Kroopnick*, 1985; *Druffel*, 1997; *Gruber et al*., 1999] and consequently influence $\delta^{13}C$ levels preserved in coral skeletons. Seasonal variability of $\delta^{13}C$ levels (0.8‰ to 1.3‰) in seawater DIC has been observed in the Caribbean Sea along the southwest coast of Puerto Rico and is driven by seasonal changes in the input of river water depleted in $\delta^{13}C$ [*Watanabe et al*., 2002]. Moreover, coral studies offshore of Florida (USA) have demonstrated that the variability in the $\delta^{13}C$ of seawater DIC and coral skeletons is similar in both timing and magnitude [*Swart et al*., 1996b]. These studies suggest that changes in the $\delta^{13}C$ levels of seawater DIC may be an important factor controlling $\delta^{13}C$ variations in coral.

[5] There have been several studies of coral $\delta^{13}C$ levels and its climatic and/or environmental implications in the South China Sea (SCS). A study near Nansha Island in the southern SCS indicated that correlations between coral $\delta^{13}C$ and environmental parameters (e.g., solar insolation, cloud cover, and rainfall) were weak ($r < 0.45$), suggesting that a variety of factors control coral $\delta^{13}C$ in this region [*Yu et al*., 2002]. Studies near Hainan Island in the northern SCS concluded that seasonal changes in coral $\delta^{13}C$ were in phase with changes in solar radiation [*Shimamura et al*., 2008; *Sun et al*., 2008]. However, in fringing reefs such as those off the coast of Hainan Island, the factors influencing coral $\delta^{13}C$ may be more complicated, particularly as river runoff appears to significantly influence the $\delta^{13}C$ of seawater DIC here [*Swart et al*., 1996, 1996b; *Moyer and Grottoli*, 2011; *Moyer et al*., 2012]. Consequently, coral $\delta^{13}C$ may reflect changes in the $\delta^{13}C$ of seawater DIC produced by changes in river runoff. *Shimamura et al*. [2008] concluded that the seasonal change in the $\delta^{13}C$ (−1.0‰ to 0.9‰) of seawater DIC was not a primary factor controlling $\delta^{13}C$ (−5.0‰ to −0.8‰) of coral from the coast of Hainan Island. However, this conclusion was based on limited monitoring data (9 months) and, critically, did not include data from July to September, when rainfall peaks in this region. Based on our previous studies, it is likely that river runoff associated with rainfall during this season on Hainan Island influences the chemistry of coastal seawater, including sea surface salinity and $\delta^{18}O$ [*Wei et al*., 2000; *Deng et al*., 2009]. Therefore, the impact of changes in the $\delta^{13}C$ of seawater DIC on coral $\delta^{13}C$ cannot be assumed to be negligible in this region.

[6] In this study, we present $\delta^{13}C$ records of corals (*Porites lutea*) from the fringing reefs of southern Hainan Island in the northern SCS. The relationships between coral skeletal $\delta^{13}C$ and environmental variables, such as solar insolation, seawater $\delta^{18}O$, temperature, rainfall, and the $\delta^{13}C$ of DIC, are then examined to determine the response of coral $\delta^{13}C$ to different climatic and environmental factors.

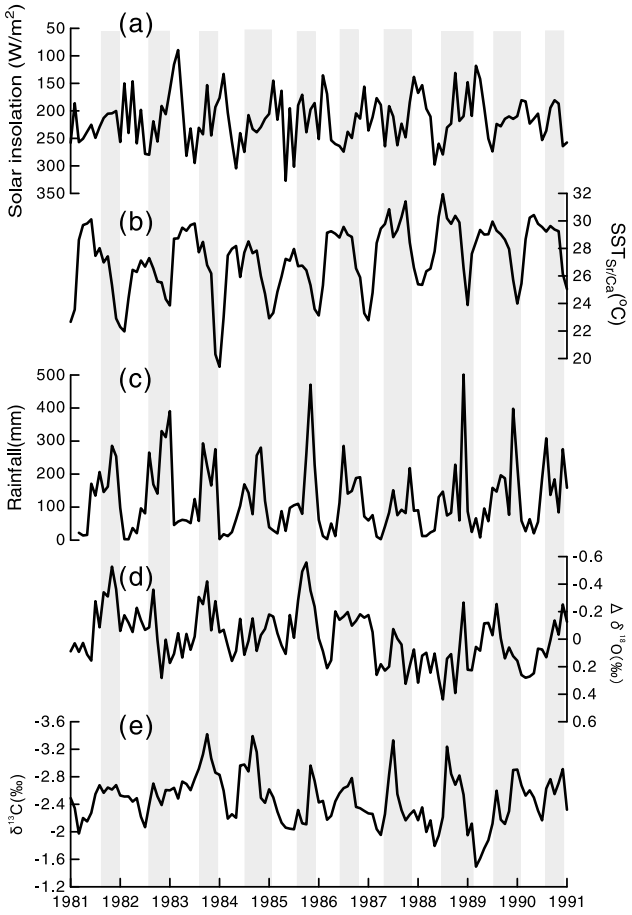

Figure 2. Monthly variations in modern coral skeletal $\delta^{13}C$ and other environmental variables. Note that $\delta^{13}C$ and $\Delta\delta^{18}O$ are plotted on an inverted scale on the *y* axis to allow a direct comparison with rainfall. The solar insolation and rainfall records were obtained from the China Meteorological Data Sharing Service System (http://cdc.cma.gov.cn/) and were calculated by averaging the rainfall records from the Haikou, Dongfang, and Qionghai meteorological observatories. Variations in coral $\delta^{13}C$ and solar insolation are out of phase, with the coral $\delta^{13}C$ maxima generally occurring from March to April and the solar insolation maxima generally occurring from May to July. The rainfall record was backdated by 2 months to align it with the $\delta^{13}C$ and $\Delta\delta^{18}O$ data. The SST record was reconstructed using the coral Sr/Ca record.

2. Materials and Methods

2.1. Coral Sampling

[7] Samples of modern and mid-Holocene *Porites lutea* corals were collected from the fringing reefs off the coast of southern Hainan Island in the northern SCS. The modern coral (SYA) was collected from Sanya Bay (18°13′N, 109° 30′E), and the mid-Holocene coral (SYO-15) was collected from Dadonghai (18°12′N, 109°33′E). The sampling locations are shown in Figure 1. Information regarding the reefs and the physical environment around the sampling locations can be found in our previous studies [*Wei et al*., 2007; *Deng et al*., 2009]. The age of SYO-15 was determined by thermal ionization mass spectrometry and the ^{238}U-^{234}U-^{230}Th method to be 6494 ± 24 year B.P. [*Wei et al*., 2007], using procedures described by *Zhao and Yu* [2002].

[8] Both the modern and mid-Holocene corals were cut using a diamond saw into slabs, 5–7 cm wide and 1 cm thick, along the major growth axis. X-radiographs were taken of the slabs to identify growth bands, which revealed that the annual growth increments ranged from 15 to 18 mm in thickness (average = 16 mm). Dark (high density) and light (low density) bands were clear within the annual growth bands in the X-radiographs [*Deng et al*., 2009], indicating different growth rates during winter and summer. No signs of diagenesis or cessation of growth were observed in the corals [*Wei et al*., 2007]. Subsamples for geochemical analysis were manually collected from the corals using a very thin and sharp surgical blade along the maximum growth axis. The average sampling interval for the geochemical analysis was around 0.6–0.8 mm, which corresponds to an approximately monthly resolution for winter growth, and a resolution of 2–3 weeks during the summer period. Sr/Ca, $\delta^{13}C$, and $\delta^{18}O$ measurements were completed on all subsamples. The Sr/Ca and $\delta^{18}O$ data for the modern and the mid-Holocene coral were previously reported in *Deng et al*. [2009].

2.2. Water Sampling

[9] From January to December 2011, seawater samples for DIC $\delta^{13}C$ analysis were collected at weekly intervals from the reef where the modern coral was sampled. The in situ sea surface salinity (SSS) was also measured when the water samples were collected. Time of day can influence the concentration and $\delta^{13}C$ of seawater DIC in shallow reef environments due to diurnal variations in net production [*Bass et al*., 2012; *Falter et al*., 2013]. To prevent any effects related to differences in sampling times, the seawater samples were collected at the same time (8:00 am local time) on each sampling day. The weekly data were averaged to give a monthly resolution series. The samples were filtered in the field through a cellulose acetate membrane with a porosity of 0.45 μm by pressure filtration, stored in precleaned 20 mL high-quality borosilicate glass bottles with a gastight rubber septum (CNW Technologies GmbH, Germany) and treated with $HgCl_2$ to prevent microbial activity.

2.3. Stable Isotope Analyses

[10] Coral skeletal $\delta^{13}C$ and $\delta^{18}O$ data were obtained using a GV Isoprime II stable isotope ratio mass spectrometer (IRMS) coupled with an online carbonate preparation system (MultiPrep) at the State Key Laboratory of Isotope Geochemistry, Guangzhou Institute of Geochemistry, Chinese Academy of Sciences, Guangzhou, China. In an individual reaction vessel in the MultiPrep system, around 0.1 mg of each sample was reacted with 102% H_3PO_4 (specific gravity = 1.92 g/cm^3) in a vacuum at a constant temperature of 90°C. The liberated CO_2 was collected and purified using liquid nitrogen cold traps and then transferred via an online dual inlet system to the IRMS. $\delta^{13}C$ and $\delta^{18}O$ values are reported as the per mil (‰) deviation of $^{13}C/^{12}C$ and $^{18}O/^{16}O$, respectively, relative to the Vienna Pee Dee belemnite (V-PDB). Approximately 15% of the samples were run in duplicate. External precisions for $\delta^{13}C$ and $\delta^{18}O$ were $< \pm 0.03‰$ (1σ) and ± 0.06‰ (1σ) ($n = 360$), respectively, as determined by repeated measurements of the international carbonate standard NBS-19 and Chinese national standard GBW04405.

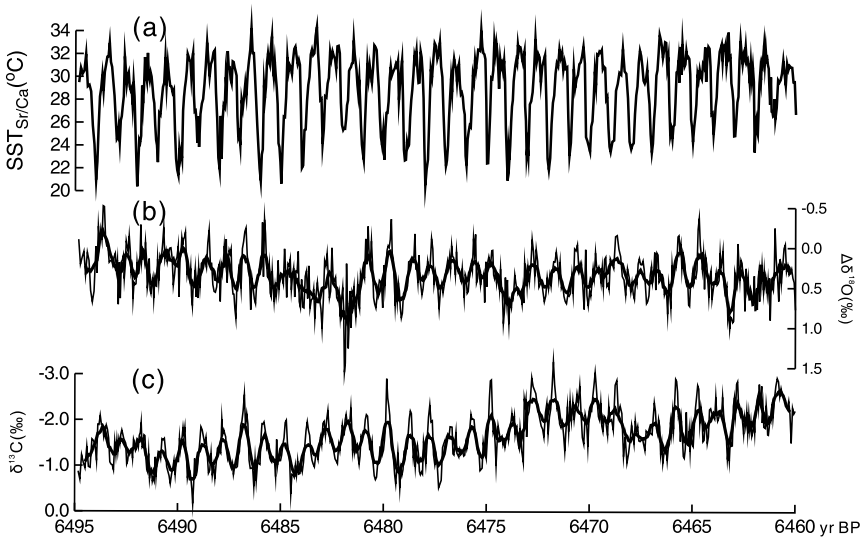

Figure 3. Temporal variations in $\delta^{13}C$-, $\Delta\delta^{18}O$-, and Sr/Ca-derived SST obtained from the mid-Holocene coral. Note that $\delta^{13}C$ and $\Delta\delta^{18}O$ are plotted on an inverted scale on the *y* axis to allow a direct comparison with Sr/Ca-derived SST. Both $\delta^{13}C$ and $\Delta\delta^{18}O$ exhibit significant annual periodicity, and these variations are mostly in phase with $\delta^{13}C$ minima and generally correspond to $\Delta\delta^{18}O$ minima. Variations in both $\delta^{13}C$ and $\Delta\delta^{18}O$ lead those of the Sr/Ca-derived SST. The bold lines representing $\delta^{13}C$ and $\Delta\delta^{18}O$ are nine-point moving averages, which highlight the synchronous variations in coral $\delta^{13}C$ and $\Delta\delta^{18}O$.

[11] The $\delta^{13}C$ values of DIC in the seawater samples were measured on an Isoprime 100 stable IRMS coupled with an online continuous flow preparation system (MultiFlow) in the same laboratory used for the other stable isotope measurements. Approximately 0.5 mL of seawater was injected into a glass vial and flushed with 99.999% purity helium gas at 38 mL/min for 200 s. Three drops of 102% H_3PO_4 were added to react with the seawater. The vials were kept at 40°C, and the reaction and equilibration were conducted for 4 h. The released CO_2 was injected into a loop, purified by a column held at a constant temperature of 90°C (Poraplot Q, 25 m × 0.32 mm, Varian Ltd), dried with a Nafion membrane, and finally carried to the stable IRMS by helium gas flow. The $\delta^{13}C$ values for DIC are also reported as the per mil (‰) deviation relative to the V-PDB standard. All samples were analyzed in duplicate. Repeated measurement of a seawater DIC working standard yielded a precision of less than ±0.1‰ (1σ) ($n = 50$).

2.4. Age Model

[12] The growth chronologies of the corals were constructed using Sr/Ca ratios, which track changes in ambient water temperature, assuming each Sr/Ca cycle represents 1 year, and by cross-validating this approach with visual observations from the X-radiographs, as the pairs of high- and low-density bands represent annual growth [*Knutson et al*., 1972; *Dodge and Vaisnys*, 1975]. Maxima in Sr/Ca ratios were assigned to the beginning (1 January) of each year, which is generally the coldest period in this region. Other ages were obtained by linear interpolation between these age control points. In the case of the modern coral, the age assignment began at the top of the core with the tissue layer, whose age was known from the date of collection (16 January 1991) of the core. For the fossil coral, the age assignment was based on seasonal cycles in Sr/Ca ratios and the U-series age. Values of $\Delta\delta^{18}O$, representing the influence of freshwater runoff, were calculated as the residual $\delta^{18}O$ value obtained by subtracting the temperature contribution from the coral $\delta^{18}O$ [*McCulloch et al*., 1994; *Gagan et al*., 1998]. Calendar ages were assigned to the $\delta^{13}C$ and $\Delta\delta^{18}O$ data over the life-span of the corals according to the age models outlined above based on the Sr/Ca cycles.

2.5. Climatic and Environmental Records

[13] Solar insolation records were obtained from the Sanya Meteorological Observatory and can be downloaded from the China Meteorological Data Sharing Service System (http://cdc.cma.gov.cn). Rainfall records for Hainan Island were based on the average rainfall recorded at the Haikou, Dongfang, and Qionghai meteorological observatories, and these are also available from the China Meteorological Data Sharing Service System (http://cdc.cma.gov.cn).

2.6. Time Offset Estimation

[14] The time offset between the coral $\delta^{13}C$ variations and the climate or paleoclimate records is important if we are to understand the response of coral $\delta^{13}C$ to environmental changes, because time offsets (leads and lags) between the records can be used to constrain the mechanism(s) forcing the geochemical changes. We used two methods to determine the extent of these time offsets. The first is the phase angle of a cross-spectral analysis between two time series records with an annual frequency. As all of our records have robust annual periodicity, variations in the phase angle can be used to quantify the leads and lags. We conducted cross-spectral analysis using the software SPECTRUM [*Schulz and Stattegger*, 1997], which is widely used in paleoclimate studies. The second method used to determine the time offsets involved showing seasonal variation in monthly means to highlight seasonal variations within a year. The monthly

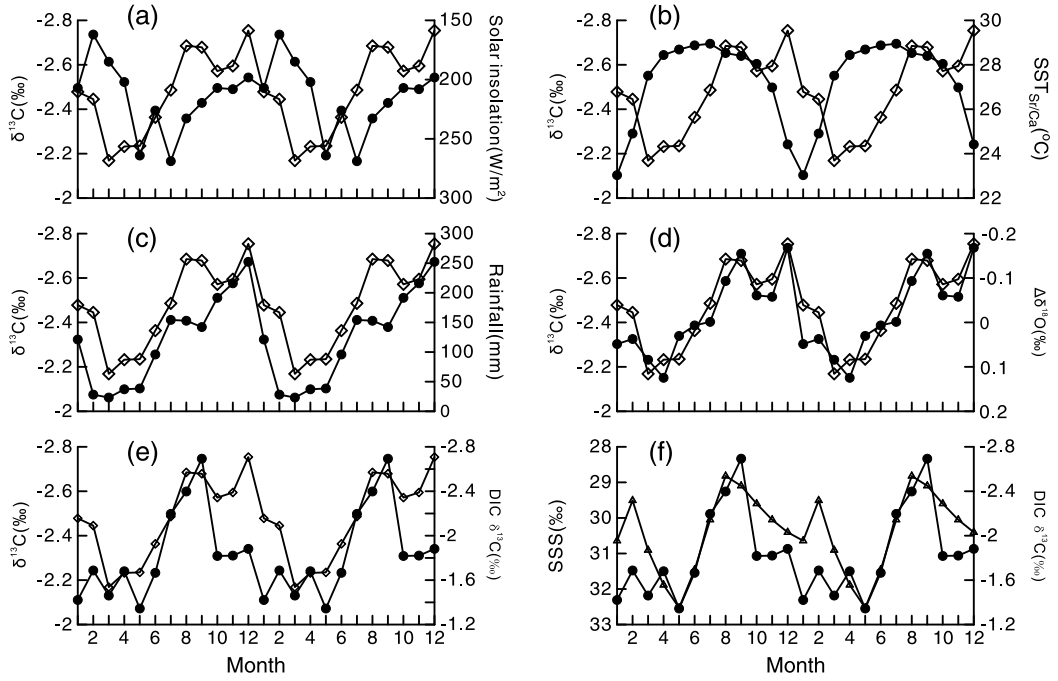

Figure 4. Modern time series showing seasonal variations in monthly means of climatic and environmental variables, and coral stable isotope data. Note that $\delta^{13}C$ and $\Delta\delta^{18}O$ are plotted on an inverted scale on the *y* axis to allow direct comparison with the other data. The solid lines with open diamond symbols represent the coral $\delta^{13}C$ data. The solid lines with open triangle and solid circle symbols represent other variables. To highlight the lead and lag relationships, two identical annual cycles of monthly mean variations in these records are presented. (a) Coral $\delta^{13}C$ and solar insolation, (b) modern coral $\delta^{13}C$ and SST, (c) coral $\delta^{13}C$ and rainfall (the rainfall was backdated by 2 months), (d) coral $\delta^{13}C$ and $\Delta\delta^{18}O$, (e) coral $\delta^{13}C$ and seawater DIC $\delta^{13}C$, and (f) seawater DIC $\delta^{13}C$ and SSS. Solar insolation and rainfall records are the same as those in Figure 2. The monthly $\delta^{13}C$ values of seawater DIC and SSS were calculated by averaging the data obtained at a weekly resolution during 2011. The $\delta^{13}C$ values of seawater DIC and SSS were not obtained during growth of the modern coral.

means of a time series were calculated by converting the series to a monthly resolution, and then averaging the data for each month across the whole series. Monthly resolution was obtained by linear interpolation (for an annual cycle with <12 data points) or nearest neighbor smoothing (for an annual cycle with >12 data points). These two methods have been adopted and described in our previous studies [e.g., *Deng et al*., 2009].

3. Results

[15] Annual periodicities are exhibited in both the modern and mid-Holocene $\delta^{13}C$ records (Figures 2 and 3, respectively). Skeletal $\delta^{13}C$ values vary from $-3.50‰$ to $-1.31‰$ and $-3.28‰$ to $-0.17‰$ for the modern and mid-Holocene corals, respectively. The average skeletal $\delta^{13}C$ values of the modern and mid-Holocene corals are $-2.47‰$ (1 SD: 0.36) and $-1.63‰$ (1 SD: 0.54), respectively.

[16] The monthly mean skeletal $\delta^{13}C$ variations of both the modern and mid-Holocene corals (Figures 4 and 5) range from $-2.75‰$ to $-2.17‰$, and from $-2.16‰$ to $-1.27‰$, respectively. In the case of the modern coral, the most negative values characterize the summer to autumn period (July to October), while the most positive values characterize March to April. However, for the mid-Holocene coral, the most

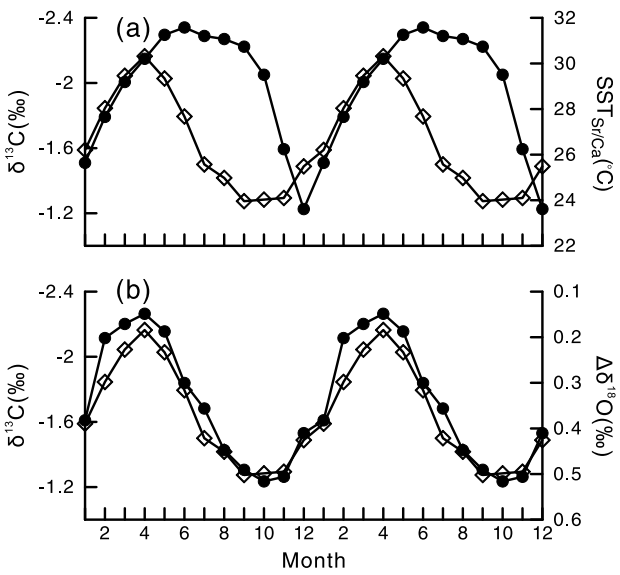

Figure 5. Time series records of the mid-Holocene coral skeletal $\delta^{13}C$, $\Delta\delta^{18}O$, and SST. The data-processing method used was the same as that in Figure 4. (a) Coral $\delta^{13}C$ and Sr/Ca-SST and (b) coral $\delta^{13}C$ and $\Delta\delta^{18}O$.

negative values characterize March to May, and the most positive values characterize September to December. The corresponding solar insolation, rainfall, coral $\Delta\delta^{18}O$, and SST derived from coral Sr/Ca ratios are plotted with the coral $\delta^{13}C$ in Figures 4 and 5. Changes in the monthly $\delta^{13}C$ levels of seawater DIC and SSS during 2011 are also presented in Figure 4. The monthly $\delta^{13}C$ of seawater DIC was calculated by averaging the 4 weeks data from each month, which varied from −2.69‰ to −1.34‰, and displays seasonal variation, with more negative values in a wet summer and autumn and less negative values in a dry winter and spring. To highlight the lead and lag relationships, two identical annual cycles of monthly mean variations in these records are presented. Time offsets between the variations in the coral skeletal $\delta^{13}C$ levels and solar insolation (cloud cover), rainfall, and SST are evident. In contrast, $\delta^{13}C$ and $\Delta\delta^{18}O$ variations were in phase for both the modern and the mid-Holocene corals.

4. Discussion

4.1. Relationships Between Coral Skeletal $\delta^{13}C$ and Climatic and Environmental Variables

4.1.1. Solar Insolation

[17] Solar insolation can influence the photosynthesis of endosymbiotic zooxanthellae in coral polyps and hence affect coral skeletal $\delta^{13}C$ levels due to metabolic fractionation [*McConnaughey*, 1989]. In general, photosynthesis of endosymbiotic zooxanthellae preferentially consumes $^{12}CO_2$, resulting in ^{13}C enrichment of the DIC in the internal calcification pool. Increased solar insolation may enhance the duration of photosynthesis, thereby resulting in higher $\delta^{13}C$ levels in the coral skeleton [*Weil et al*., 1981; *Grottoli and Wellington*, 1999]. Variations of $\delta^{13}C$ in the modern coral and the observed solar insolation in this region are shown in Figure 2. Both $\delta^{13}C$ and solar insolation show similar annual periodicities. However, these variations are not in phase, with the coral $\delta^{13}C$ maxima generally occurring from March to April, and the solar insolation maxima generally occurring from May to July (Figure 2). Hence, the overall correlation between solar insolation and coral $\delta^{13}C$ is poor ($r = 0.01$, $n = 121$, $p = 0.46$) (Table 1). Seasonal variation in monthly means also shows that the coral $\delta^{13}C$ variations generally lead those of solar insolation by around 2 months (Figure 4a). This relationship has also been observed in modern *Porites* corals from Yongshu Reef, in the Nansha Islands of the southern SCS [*Yu et al*., 2002]. The $\delta^{13}C$ maxima in coral reflect the maximum net productivity of zooxanthellae photosynthesis. Figure 4a shows that coral $\delta^{13}C$ levels reach a productivity maximum around 2 months before the solar maximum. Thus, the apparent lead of coral $\delta^{13}C$ levels ahead of solar insolation indicates that this variable is not a key driver of coral $\delta^{13}C$ variations. In addition, coral $\delta^{13}C$ variations do not appear to respond linearly to solar insolation. This is consistent with the fact that overexposure to solar radiation during solar insolation maxima does not benefit the growth of zooxanthellae [*Grottoli*, 2002; *Yu et al*., 2002].

4.1.2. Sea Surface Temperature

[18] Previous studies have suggested that SST may affect coral $\delta^{13}C$ by influencing the photosynthesis of symbiotic zooxanthellae [*McConnaughey*, 1989; *Swart et al*., 1996b]. Here, the correlation between coral $\delta^{13}C$ and SST in the modern ($r = 0.07$, $n = 121$, $p = 0.22$) and mid-Holocene corals ($r = -0.01$, $n = 657$, $p = 0.40$) was poor (Table 1). The phase angles of a cross-spectral analysis between coral $\delta^{13}C$ and SST at an annual frequency were $-76 \pm 11°$ and $103 \pm 6°$ in the modern and mid-Holocene corals, respectively. These results indicate that the $\delta^{13}C$ variations lag SST by about 2.5 months during modern times but led SST by approximately 3.4 months during the mid-Holocene. These time offsets are the same as those between the coral $\Delta\delta^{18}O$ and SST [*Deng et al*., 2009], which suggests that coral $\Delta\delta^{18}O$ and $\delta^{13}C$ may exert same dominant controlling factor. Furthermore, there are well-defined time offsets between the SST and coral $\delta^{13}C$ monthly mean records (Figures 4b and 5a). The correlations between these two monthly mean records are also very weak and not significant (Table 2; $r = 0.17$, $n = 12$, $p = 0.30$ for the modern coral, and $r = 0.20$, $n = 12$, $p = 0.27$ for the mid-Holocene coral). Warm seasons typically favor coral growth, and thus, higher temperatures may enhance zooxanthellae photosynthesis and result in higher coral $\delta^{13}C$ levels [*Swart et al*., 1996b]. The weak correlation between SST and $\delta^{13}C$ seems to support this interpretation. However, this correlation is not significant; therefore, the controlling effect of SST on seasonal coral $\delta^{13}C$ in this region may not be important either.

4.1.3. Rainfall

[19] Rainfall does not influence coral $\delta^{13}C$ directly, but it enhances river runoff that can, in turn, transport significant amounts of DIC to coastal regions. Given that DIC in river water generally has a more negative $\delta^{13}C$value than seawater, enhanced river runoff may decrease the $\delta^{13}C$ of DIC in coastal seawater and so reduce the $\delta^{13}C$ levels of the coral skeletons [*Swart et al*., 1996b; *Watanabe et al*., 2002]. Variations of $\delta^{13}C$ in the modern coral and the observed rainfall record on Hainan Island (Figure 2) both exhibit similar variations with robust annual periodicities. Negative $\delta^{13}C$ peaks generally correspond to rainfall maxima, which suggest that rainfall is driving the variations in the coral $\delta^{13}C$. However, the variations of these two records are not synchronous, and coral $\delta^{13}C$ variations generally lag rainfall variations (note that the rainfall record shown in Figure 2c has been backdated by 2 months to match the $\delta^{13}C$ record). The phase angle at the annual frequency between these two records is $-51 \pm 9°$, indicating a lag of approximately 2 months in coral $\delta^{13}C$ variations relative to rainfall variations on Hainan Island. In addition, if the time offset is compensated for by adjusting the rainfall record backwards by 2 months, their correlation is much improved: from $r = -0.07$ (Table 1; $n = 121$, $p = 0.22$) to $r = -0.38$ ($n = 121$, $p < 0.00001$). This lag is also seen in the seasonal variation of the monthly means of these two records (Figure 4c). This correlation can also be observed in the monthly mean seasonal rainfall and $\delta^{13}C$ variations. After the rainfall record was adjusted backwards by 2 months, the correlation of their monthly means was much improved: from $r = -0.53$ ($n = 12$, $p = 0.038$) to $r = -0.86$ ($n = 12$, $p = 0.0002$) (Table 2).

[20] This time offset of approximately 2 months is the same as that observed between coral $\Delta\delta^{18}O$ and rainfall variations [*Deng et al*., 2009] and is also in accord with the observed lag of about 2 months between changes in seawater salinity off the southern coast of Hainan Island and rainfall on Hainan Island [*Wei et al*., 2000; *Deng et al*., 2009]. Figures 2d and 2e highlight that $\Delta\delta^{18}O$ and $\delta^{13}C$ variations

Table 1. Correlations Between Monthly Resolution Coral $\delta^{13}C$ Values and Other Environmental Variables

	Solar Insolation	$SST_{Sr/Ca}$	Rainfall[a]	Rainfall[b]	$\Delta\delta^{18}O$
Modern coral $\delta^{13}C$	$r = 0.01$ $n = 121$ $p = 0.46$	$r = 0.07$ $n = 121$ $p = 0.22$	$r = -0.07$ $n = 121$ $p = 0.22$	$r = -0.38$ $n = 121$ $p < 0.00001$	$r = 0.26$ $n = 121$ $p = 0.002$
Mid-Holocene coral $\delta^{13}C$	–	$r = -0.01$ $n = 657$ $p = 0.40$	–	–	$r = 0.24$ $n = 657$ $p < 0.0000001$

[a]Normal rainfall record.
[b]Rainfall record adjusted backwards by 2 months.

are in phase, and these two data sets are positively correlated (Table 1; $r = 0.26$, $n = 121$, $p = 0.002$). The phase angle of a cross-spectral analysis between $\Delta\delta^{18}O$ and $\delta^{13}C$ at an annual frequency is $7° \pm 7°$, highlighting the synchronicity of these two records. The synchronicity of these two records is also evident in the seasonal variation of their monthly means (Figure 4d), which are highly correlated (Table 2; $r = 0.87$, $n = 12$, $p = 0.0001$). Coral $\Delta\delta^{18}O$ has been shown to be a proxy for rainfall changes on Hainan Island [*Deng et al*., 2009]. The similar time offset of the coral $\delta^{13}C$ and $\Delta\delta^{18}O$ records when compared with the rainfall variations suggests that the variations in coral $\delta^{13}C$ levels were associated with rainfall patterns on Hainan Island.

[21] The relationship between coral $\delta^{13}C$ and rainfall in this region is evident both in the modern and mid-Holocene corals. As there is no measured rainfall record from the mid-Holocene, coral $\Delta\delta^{18}O$ is used here as a proxy for variations in rainfall amounts [*Deng et al*., 2009]. Variations in $\delta^{13}C$ and $\Delta\delta^{18}O$ from the mid-Holocene coral are shown in Figures 3b and 3c, and both exhibit a significant annual periodicity. The variations are generally in phase, with $\delta^{13}C$ maxima and minima corresponding to those of $\Delta\delta^{18}O$, and these two variables display a positive correlation (Table 1; $r = 0.24$, $n = 657$, $p < 0.0000001$). The phase angle of a cross-spectral analysis between $\delta^{13}C$ and $\Delta\delta^{18}O$ records is $-12° \pm 10°$, showing that the variations in these records are almost synchronous. This is supported by the monthly mean $\delta^{13}C$ and $\Delta\delta^{18}O$ records (Figure 5b), which are highly correlated (Table 2; $r = 0.98$, $n = 12$, $p < 0.0000001$). The above observations all strongly suggest that variations in the $\delta^{13}C$ preserved in corals from Sanya were driven primarily by variations in rainfall on Hainan Island during the mid-Holocene.

[22] The link between variations in rainfall and coral $\delta^{13}C$ is most likely to be related to river inputs to the ocean [*Moyer and Grottoli*, 2011; *Moyer et al*., 2012], as the rainwater contributes significantly to river runoff and influences the abundance, composition, and timing of carbon discharge to the coastal ocean [*Moyer and Grottoli*, 2011; *Moyer et al*., 2012]. Carbon depleted in ^{13}C derived from decomposition of terrestrial organic matter [*Raymond et al*., 2004; *Mayorga et al*., 2005] results in the DIC of river water generally showing a larger variation range and more negative $\delta^{13}C$ (typically 0‰ to −26‰) than surface seawater (typically 1‰ to 3‰). There have been no direct measurements of the $\delta^{13}C$ of DIC in river water around Sanya. However, the $\delta^{13}C$ of DIC in river water from Xijiang River (south China) ranges from −12.96‰ to −6.59‰ [*Wei et al*., 2013]. It is evident that the $\delta^{13}C$ during the rainy summer and autumn period is generally more negative, by about 2‰ to 3‰, than during the dry spring and winter [*Wei et al*., 2013]. A similar pattern of $\delta^{13}C$ variations in the DIC of rivers around Sanya can be assumed, because the two sites are close and have similar geological and environmental backgrounds, where enhanced rainfall during the rainy season increases river runoff and this transports larger amounts of DIC, with a more negative $\delta^{13}C$, to the coastal coral reefs. In turn, this results in a decrease in the $\delta^{13}C$ of seawater DIC and, consequently, in reduced coral $\delta^{13}C$ levels [*Moyer and Grottoli*, 2011; *Moyer et al*., 2012].

[23] This assumption is further supported by the $\delta^{13}C$ of seawater DIC and SSS in the region of Sanya coral reef, which was monitored during 2011. Figures 4e and 4f show that the $\delta^{13}C$ of seawater DIC varied from −2.69‰ to −1.34‰, the SSS varied from 28.82‰ to 32.53‰, and these changes were closely tracked by those in the modern coral. The correlation between the $\delta^{13}C$ of seawater DIC and that of the coral is significant (Table 2; $r = 0.69$, $n = 12$, $p = 0.007$). The correlation between the $\delta^{13}C$ of seawater DIC and SSS is also significant (Table 2; $r = 0.74$, $n = 12$, $p = 0.003$). Although the seawater DIC $\delta^{13}C$ and SSS records are relatively short and the monitoring was not conducted during the growth of the coral, it is reasonable to assume that the historical, seasonal $\delta^{13}C$ variations of seawater DIC and SSS should be similar and that changes in the $\delta^{13}C$ of seawater DIC control $\delta^{13}C$ variations in corals in this region. In summary, this supports our arguments outlined above that

Table 2. Correlations Between Monthly Means of Coral $\delta^{13}C$ Values and Other Environmental Variables

	Solar Insolation	$SST_{Sr/Ca}$	Rainfall[a]	Rainfall[b]	$\Delta\delta^{18}O$	SeawaterDIC ^{13}C
Modern coral $\delta^{13}C$	$r = 0.002$ $n = 12$ $p = 0.49$	$r = 0.17$ $n = 12$ $p = 0.30$	$r = -0.53$ $n = 12$ $p = 0.038$	$r = -0.86$ $n = 12$ $p = 0.0002$	$r = 0.87$ $n = 12$ $p = 0.0001$	$r = 0.69$ $n = 12$ $p = 0.007$
Mid-Holocene coral $\delta^{13}C$	–	$r = 0.20$ $n = 12$ $p = 0.27$	–	–	$r = 0.98$ $n = 12$ $p < 0.0000001$	–

[a]Normal rainfall record.
[b]Rainfall record adjusted backwards by 2 months.

variations in coral $\delta^{13}C$ are associated with rainfall patterns in this region.

4.2. Main Factors Controlling Coral Skeletal $\delta^{13}C$ in the Coastal SCS

[24] Changes in the $\delta^{13}C$ of seawater produced by river runoff have not generally been considered an important influence on coral $\delta^{13}C$ levels. Although *Swart et al.* [1996a] attributed changes in coral $\delta^{18}O$ from south Florida (USA) to fresh water outflow associated with rainfall from the mainland, it was not considered to be the primary factor driving coral $\delta^{13}C$ variations, given the poor correlation between coral $\delta^{13}C$ and rainfall. The absence of a correlation between coral $\delta^{13}C$ and rainfall records can potentially be attributed to the time offset between the peaks of rainfall on land and chemical changes in coastal seawater. Coastal seawater is not always immediately diluted when heavy rainfall occurs over nearby land. For example, the observed seawater salinity minimum off the southern coast of Hainan Island generally lags peak rainfall on Hainan Island by around 2 months [*Wei et al.*, 2000; *Deng et al.*, 2009]. Considering this observation, and by comparing the $\delta^{13}C$ and $\Delta\delta^{18}O$ variations, as well as allowing for the probable time offset between rainfall and seawater salinity change, we conclude that river runoff associated with rainfall is the primary factor controlling coral $\delta^{13}C$ in this region.

[25] To estimate the contribution of the riverine DIC to the overall coral $\delta^{13}C$ signature, a simple mass balance model suggested by *Moyer and Grottoli* [2011] was constructed using the equation: $\delta^{13}C_{coral} = x\delta^{13}C_{rw} + (1 - x)\ \delta^{13}C_{sw}$. In this equation, x is the unknown proportion being solved for, $\delta^{13}C_{coral}$ is the average $\delta^{13}C$ minima (wet season, -3.03 ± 0.26‰) and maxima (dry season, -2.03 ± 0.29‰) for the entire coral record, $\delta^{13}C_{rw}$ is the average riverine water end-member DIC $\delta^{13}C$ values during the wet or dry season (-9.20‰ or -7.11‰) based on the Xijiang River data [*Wei et al.*, 2013], and $\delta^{13}C_{sw}$ is the average of DIC $\delta^{13}C$ in the offshore waters of the northern SCS during the wet or dry season. The averages of DIC $\delta^{13}C$ in the offshore waters in the northern SCS during the wet and dry season are very similar and close to 0.5‰ [*Liu*, 2005]. All data processing followed the method of *Moyer and Grottoli* [2011]. The mass balance results revealed that during the wet season the proportionate contribution of riverine DIC $\delta^{13}C$ to the coral $\delta^{13}C$ minima was 36.3 ± 3.4%. During the dry season, the proportionate contribution of riverine DIC $\delta^{13}C$ to the coral $\delta^{13}C$ maxima was 33.2 ± 4.3%. Thus, the seasonal cycle of riverine DIC input to the coastal northern SCS appears to be the main factor affecting the annual periodicity observed in coral skeletal $\delta^{13}C$ by influencing the DIC $\delta^{13}C$ in ambient seawater. Both contributions during dry and wet seasons are higher than those in Puerto Rico reported by *Moyer and Grottoli* [2011], which suggests that the contribution of riverine DIC $\delta^{13}C$ to the coral $\delta^{13}C$ in the northern SCS may be more significant.

[26] Prior experiments indicate that changes in zooxanthellar productivity and respiration can alter coral skeletal $\delta^{13}C$ by 0.5‰ to 1.0‰ [*Grottoli and Wellington*, 1999; *Grottoli*, 2002]. In the northern SCS, we observe changes on the order of 2‰ (Figure 2e). However, the coral $\delta^{13}C$ maxima generally occur around March–April, while the observed productivity maxima generally occur in summer, when light levels and temperature are highest [*Huang et al.*, 2003]. The $\delta^{13}C$ levels of the SCS coral are not well correlated with either solar insolation or temperature but are well correlated with runoff associated with the rainfall (albeit it with a time lag of 2 months). In addition, the $\delta^{13}C$ values of all modern corals (-0.72‰ to -5.41‰) from fringing reefs in this study, and also two other studies in the northern SCS [*Shimamura et al.*, 2008; *Sun et al.*, 2008], are more depleted than those of other coral reefs from the southern SCS that are unaffected by river runoff. For example, $\delta^{13}C$ values of a modern coral from Yongshu Reef in the southern SCS range from -0.34‰ to -3.04‰ [*Yu et al.*, 2002]. This difference between coral $\delta^{13}C$ values can be mostly attributed to river runoff that lowers the baseline $\delta^{13}C$ values of DIC in ambient seawater around fringing reefs. While we cannot rule out the kinetic and equilibrium fractionation effects of zooxanthellar metabolism on the isotopic composition of coral skeletons, our results show that the dominant influence on the $\delta^{13}C$ levels of corals growing in the coastal SCS is the isotopic composition of the ambient DIC.

[27] In addition to these seasonal factors, the ^{13}C Suess effect can induce a long-term decrease in coral $\delta^{13}C$ due to the increased addition to the ocean of anthropogenic $^{12}CO_2$ produced by burning isotopically light hydrocarbons [*Swart et al.*, 2010; *Dassié et al.*, 2013]. Most coral $\delta^{13}C$ records exhibit this long-term decrease toward the present day [*Swart et al.*, 2010]. Our modern coral $\delta^{13}C$ record is relatively short and thus did not reveal this long-term trend over recent decades. However, $\delta^{13}C$ records obtained from three modern corals from the northern SCS spanning the past 15–35 years did exhibit this trend [*Sun et al.*, 2008]. Notably, $\delta^{13}C$ values of the modern coral (-3.50‰ to -1.31‰; average $= -2.47$‰) are more negative than those of the mid-Holocene coral (-3.28‰ to -0.17‰; average $= -1.63$‰) in our study, which may be explained by the ^{13}C Suess effect, indicating that this effect does change coral $\delta^{13}C$ levels over the long term in this region.

[28] Previous studies have indicated that coral $\delta^{13}C$ records the delivery of riverine DIC to the coastal ocean and can be used as a proxy for land-ocean carbon flux in tropical regions [*Moyer and Grottoli*, 2011; *Moyer et al.*, 2012]. These data, together with our findings, appear to demonstrate that $\delta^{13}C$ in coral skeletons from coastal environments are controlled mainly by terrestrial carbon input and are significantly influenced by terrestrial river runoff. As a result, the geochemical interpretations of coral $\delta^{13}C$ records may differ between coastal sites and offshore areas or the open ocean.

5. Conclusions

[29] We studied the $\delta^{13}C$ isotope systematics of modern and mid-Holocene corals from the northern SCS and examined the relationship between coral $\delta^{13}C$ and climatic and environmental variables, including solar insolation, rainfall, and SST. The main conclusions of our study are outlined below.

[30] Solar insolation and SST have a negligible effect on coral skeletal $\delta^{13}C$. However, rainfall on Hainan Island plays an important role in controlling coral $\delta^{13}C$ over seasonal time scales. River runoff from rainfall on Hainan Island enhances delivery of DIC with a more negative $\delta^{13}C$ to the coast, thereby lowering the $\delta^{13}C$ of surrounding seawater DIC and resulting in a more negative coral $\delta^{13}C$ levels.

[31] Primary productivity appears to have little effect on coral skeletal $\delta^{13}C$ levels. However, the $\delta^{13}C$ of organic material on the reef, such as zooxanthellae and coral tissues, may, in part, control the seasonal variations in coral skeletal $\delta^{13}C$. The ^{13}C Suess effect is also responsible for changes in coral $\delta^{13}C$ over long time scales in this region.

[32] Coral skeletal $\delta^{13}C$ in coastal environments are controlled mainly by terrestrial carbon input and are significantly influenced by terrestrial river runoff. Consequently, the geochemical interpretation of coral $\delta^{13}C$ records may differ between coastal areas and offshore or the open ocean.

[33] **Acknowledgments.** The authors would like to thank the Editor Dennis Baldocchi and two anonymous reviewers for their helpful comments and constructive suggestions. Allan Chivas is thanked for his valuable suggestions and discussions. The English of the manuscript was improved by Stallard Scientific Editing. This work was financially supported by the National Basic Research Program of China (2009CB421206, 2013CB956103) and the National Natural Sciences Foundation of China (41173004, 40902050, 40830852). This is contribution IS-1738. from GIGCAS.

References

Al-Horani, F. A., S. M. Al-Moghrabi, and D. de Beer (2003), The mechanism of calcification and its relation to photosynthesis and respiration in the scleractinian coral *Galaxea fascicularis*, *Mar. Biol.*, *142*(3), 419–426, doi:10.1007/s00227-002-0981-8.

Allison, N., and A. A. Finch (2012), A high resolution $\delta^{13}C$ record in a modern *Porites lobata* coral: Insights into controls on skeletal $\delta^{13}C$, *Geochim. Cosmochim. Acta*, *84*, 534–542, doi:10.1016/j.gca.2012.02.004.

Allison, N., A. W. Tudhope, and A. E. Fallick (1996), Factors influencing the stable carbon and oxygen isotopic composition of *Porites lutea* coral skeletons from Phuket, South Thailand, *Coral Reefs*, *15*(1), 43–57, doi:10.1007/BF01626076.

Atekwana, E. A., and R. V. Krishnamurthy (1998), Seasonal variations of dissolved inorganic carbon and $\delta^{13}C$ of surface water: Application of a modified gas evolution technique, *J. Hydrol.*, *205*, 265–278, doi:10.1016/S0022-1694(98)00080-8.

Bass, A. M., M. I. Bird, N. C. Munksgaard, and C. M. Wurster (2012), ISO-CADICA: Isotopic–continuous, automated dissolved inorganic carbon analyser, *Rapid Commun. Mass Spectrom.*, *26*(6), 639–644, doi:10.1002/rcm.6143.

Boiseau, M., A. Juillet-Leclerc, P. Yiou, B. Salvat, P. Isdale, and M. Guillaume (1998), Atmospheric and oceanic evidences of El Niño Southern Oscillation events in the south central Pacific Ocean from coral stable isotopic records over the last 137 years, *Paleoceanography*, *13*(6), 671–685, doi:10.1029/98PA02502.

Dassié, E. P., G. M. Lemley, and B. K. Linsley (2013), The Suess effect in Fiji coral $\delta^{13}C$ and its potential as a tracer of anthropogenic CO_2 uptake, *Paleogeogr. Paleoclimatol. Paleoecol.*, *370*(0), 30–40, doi:10.1016/j.palaeo.2012.11.012.

Deng, W. F., G. J. Wei, X. H. Li, K. F. Yu, J. X. Zhao, W. D. Sun, and Y. Liu (2009), Paleoprecipitation record from coral Sr/Ca and $\delta^{18}O$ during the mid Holocene in the northern South China Sea, *Holocene*, *19*(6), 811–821, doi:10.1177/0959683609337355.

Dodge, R. E., and J. R. Vaisnys (1975), Hermatypic coral growth banding as environmental recorder, *Nature*, *258*(5537), 706–708.

Druffel, E. R. M. (1997), Geochemistry of corals: Proxies of past ocean chemistry, ocean circulation, and climate, *Proc. Natl. Acad. Sci. U. S. A.*, *94*, 8354–8361.

Fabricius, K. E. (2005), Effects of terrestrial runoff on the ecology of corals and coral reefs: Review and synthesis, *Mar. Pollut. Bull.*, *50*(2), 125–146, doi:10.1016/j.marpolbul.2004.11.028.

Fairbanks, R. G., and R. E. Dodge (1979), Annual periodicity of the $^{18}O/^{16}O$ and $^{13}C/^{12}C$ ratios in the coral *Montastrea annularis*, *Geochim. Cosmochim. Acta*, *43*(7), 1009–1020, doi:10.1016/0016-7037(79)90090-5.

Falter, J. L., R. J. Lowe, Z. L. Zhang, and M. McCulloch (2013), Physical and biological controls on the carbonate chemistry of coral reef waters: Effects of metabolism, wave forcing, sea level, and geomorphology, *Plos One*, *8*(1), e53303, doi:10.1371/journal.pone.0053303.

Furla, P., D. Allemand, and M. N. Orsenigo (2000), Involvement of H^+-ATPase and carbonic anhydrase in inorganic carbon uptake for endosymbiont photosynthesis, *Am. J. Physiol.-Regul. Integr. Comp. Physiol.*, *278*(4), R870–R881.

Furnas, M. J. (2003), *Catchments and corals: Terrestrial runoff to the Great Barrier Reef*, Australian Institute of Marine Science Townsville, Queensland, Australia.

Gagan, M. K., A. R. Chivas, and P. J. Isdale (1994), High-resolution isotopic records from corals using ocean temperature and mass-spawning chronometers, *Earth Planet. Sci. Lett.*, *121*(3–4), 549–558, doi:10.1016/0012-821X(94)90090-6.

Gagan, M. K., A. R. Chivas, and P. J. Isdale (1996), Timing coral-based climatic histories using ^{13}C enrichments driven by synchronized spawning, *Geology*, *24*(11), 1009–1012.

Gagan, M. K., L. K. Ayliffe, D. Hopley, J. A. Cali, G. E. Mortimer, J. Chappell, M. T. McCulloch, and M. J. Head (1998), Temperature and surface-ocean water balance of the mid-Holocene tropical Western Pacific, *Science*, *279*(5353), 1014–1018, doi:10.1126/science.279.5353.1014.

Gattuso, J. P., D. Allemand, and M. Frankignoulle (1999), Photosynthesis and calcification at cellular, organismal and community levels in coral reefs: A review on interactions and control by carbonate chemistry, *Amer. Zool.*, *39*(1), 160–183, doi:10.1093/icb/39.1.160.

Grottoli, A. G. (2002), Effect of light and brine shrimp on skeletal $\delta^{13}C$ in the Hawaiian coral *Porites compressa*: A tank experiment, *Geochim. Cosmochim. Acta*, *66*(11), 1955–1967, doi:10.1016/S0016-7037(01)00901-2.

Grottoli, A. G., and G. M. Wellington (1999), Effect of light and zooplankton on skeletal $\delta^{13}C$ values in the eastern Pacific corals *Pavona clavus* and *Pavona gigantea*, *Coral Reefs*, *18*(1), 29–41, doi:10.1007/s003380050150.

Gruber, N., C. D. Keeling, R. B. Bacastow, P. R. Guenther, T. J. Lueker, M. Wahlen, H. A. J. Meijer, W. G. Mook, and T. F. Stocker (1999), Spatiotemporal patterns of carbon-13 in the global surface oceans and the oceanic Suess effect, *Glob. Biogeochem. Cycle*, *13*(2), 307–335, doi:10.1029/1999GB900019.

Heikoop, J. M., J. J. Dunn, M. J. Risk, H. P. Schwarcz, T. A. McConnaughey, and I. M. Sandeman (2000), Separation of kinetic and metabolic isotope effects in carbon-13 records preserved in reef coral skeletons, *Geochim. Cosmochim. Acta*, *64*(6), 975–987, doi:10.1016/S0016-7037(99)00363-4.

Hendy, E. J., M. K. Gagan, C. A. Alibert, M. T. McCulloch, J. M. Lough, and P. J. Isdale (2002), Abrupt decrease in tropical Pacific Sea surface salinity at end of Little Ice Age, *Science*, *295*(5559), 1511–1514, doi:10.1126/science.1067693.

Huang, L., Y. Tan, X. Song, X. Huang, H. Wang, S. Zhang, J. Dong, and R. Chen (2003), The status of the ecological environment and a proposed protection strategy in Sanya Bay, Hainan Island, China, *Mar. Pollut. Bull.*, *47*(1–6), 180–186, doi:10.1016/S0025-326X(03)00070-5.

Knutson, D. W., R. W. Buddemeier, and S. V. Smith (1972), Coral chronometers: Seasonal growth bands in reef corals, *Science*, *177*(4045), 270–272.

Kroopnick, P. M. (1985), The distribution of ^{13}C of ΣCO_2 in the world oceans, *Deep-Sea Res., Part A*, *32*(1), 57–84, doi:10.1016/0198-0149(85)90017-2.

Land, L. S., J. C. Lang, and B. N. Smith (1975), Preliminary observations on the carbon isotopic composition of some reef coral tissues and symbiotic zooxanthellae, *Limnol. Oceanogr.*, *20*(2), 283–287.

Leder, J. J., A. M. Szmant, and P. K. Swart (1991), The effect of prolonged "bleaching" on skeletal banding and stable isotopic composition in *Montastrea annularis*, *Coral Reefs*, *10*(1), 19–27, doi:10.1007/BF00301902.

Liu, Q. M. (2005), The stable isotopes geochemical characteristics of dissolved inorganic carbon in the northern South China Sea and the Pearl River Estuary. Post-doctoral research report, College of Ocean and Earth Sciences, Xiamen University, Xiamen, China.

Maier, C., J. Patzold, and R. P. M. Bak (2003), The skeletal isotopic composition as an indicator of ecological and physiological plasticity in the coral genus *Madracis*, *Coral Reefs*, *22*(4), 370–380, doi:10.1007/s00338-003-0348-8.

Mayorga, E., A. K. Aufdenkampe, C. A. Masiello, A. V. Krusche, J. I. Hedges, P. D. Quay, J. E. Richey, and T. A. Brown (2005), Young organic matter as a source of carbon dioxide outgassing from Amazonian rivers, *Nature*, *436*(7050), 538–541, doi:10.1038/nature03880.

McConnaughey, T. A. (1989), ^{13}C and ^{18}O isotopic disequilibrium in biological carbonates: I. Patterns, *Geochim. Cosmochim. Acta*, *53*, 151–162, doi:10.1016/0016-7037(89)90282-2.

McConnaughey, T. A. (2003), Sub-equilibrium oxygen-18 and carbon-13 levels in biological carbonates: Carbonate and kinetic models, *Coral Reefs*, *22*(4), 316–327, doi:10.1007/s00338-003-0325-2.

McConnaughey, T. A., J. Burdett, J. F. Whelan, and C. H. Paull (1997), Carbon isotopes in biological carbonates: Respiration and photosynthesis, *Geochim. Cosmochim. Acta*, *61*(3), 611–622, doi:10.1016/S0016-7037(96)00361-4.

McCulloch, M. T., M. K. Gagan, G. E. Mortimer, A. R. Chivas, and P. J. Isdale (1994), A high-resolution Sr/Ca and $\delta^{18}O$ coral record from the Great Barrier Reef, Australia, and the 1982-1983 El-Niño, *Geochim. Cosmochim. Acta*, *58*(12), 2747–2754, doi:10.1016/0016-7037(94)90142-2.

McCulloch, M., S. Fallon, T. Wyndham, E. Hendy, J. Lough, and D. Barnes (2003), Coral record of increased sediment flux to the inner Great Barrier

Reef since European settlement, *Nature*, *421*(6924), 727–730, doi:10.1038/nature01361.

Moyer, R. P., and A. G. Grottoli (2011), Coral skeletal carbon isotopes ($\delta^{13}C$ and $\Delta^{14}C$) record the delivery of terrestrial carbon to the coastal waters of Puerto Rico, *Coral Reefs*, *30*(3), 791–802, doi:10.1007/s00338-011-0758-y.

Moyer, R. P., A. G. Grottoli, and J. W. Olesik (2012), A multiproxy record of terrestrial inputs to the coastal ocean using minor and trace elements (Ba/Ca, Mn/Ca, Y/Ca) and carbon isotopes ($\delta^{13}C$, $\Delta^{14}C$) in a nearshore coral from Puerto Rico, *Paleoceanography*, *27*, PA3205, doi:10.1029/2011PA002249.

Omata, T., A. Suzuki, T. Sato, K. Minoshima, E. Nomaru, A. Murakami, S. Murayama, H. Kawahata, and T. Maruyama (2008), Effect of photosynthetic light dosage on carbon isotope composition in the coral skeleton: Long-term culture of *Porites* spp., *J. Geophys. Res.*, *113*, G02014, doi:10.1029/02007JG000431.

Palmer, S. M., D. Hope, M. F. Billett, J. J. C. Dawson, and C. L. Bryant (2001), Source of organic and inorganic carbon in a headwater stream: Evidence from carbon isotope studies, *Biogeochemistry*, *52*, 321–338, doi:10.1023/A:1006447706565.

Porter, J. W., W. K. Fitt, H. J. Spero, and C. S. Rogers (1989), Bleaching in reef corals: Physiological and stable isotopic responses, *Proc. Natl. Acad. Sci. U. S. A.*, *86*, 9342–9346.

Quay, P. D., D. O. Wilbur, J. E. Richey, J. I. Hedges, and A. H. Devol (1992), Carbon cycling in the Amazon River: Implications from the ^{13}C compositions of particles and solutes, *Limnol. Oceanogr.*, *37*(4), 857–871.

Raymond, P. A., J. E. Bauer, N. F. Caraco, J. J. Cole, B. Longworth, and S. T. Petsch (2004), Controls on the variability of organic matter and dissolved inorganic carbon ages in northeast US rivers, *Mar. Chem.*, *92*(1–4), 353–366, doi:10.1016/j.marchem.2004.06.036.

Reynaud, S., C. Ferrier-Pages, R. Sambrotto, A. Juillet-Leclerc, J. Jaubert, and J. P. Gattuso (2002), Effect of feeding on the carbon and oxygen isotopic composition in the tissues and skeleton of the zooxanthellate coral *Stylophora pistillata*, *Mar. Ecol.-Prog. Ser.*, *238*, 81–89, doi:10.3354/meps238081.

Rosenfeld, M., R. Yam, A. Shemesh, and Y. Loya (2003), Implication of water depth on stable isotope composition and skeletal density banding patterns in a *Porites lutea* colony: Results from a long-term translocation experiment, *Coral Reefs*, *22*(4), 337–345, doi:10.1007/s00338-003-0333-2.

Schulz, M., and K. Stattegger (1997), SPECTRUM: Spectral analysis of unevenly spaced paleoclimatic time series, *Comput. Geosci.*, *23*(9), 929–945, doi:10.1016/S0098-3004(97)00087-3.

Shimamura, M., T. Irino, T. Oba, G. Q. Xu, B. Q. Lu, L. J. Wang, and K. Toyoda (2008), Main controlling factors of coral skeletal carbon isotopic composition and skeletal extension rate: High-resolution study at Hainan Island, South China Sea, *Geochem. Geophys. Geosyst.*, *9*, Q04024, doi:10.1029/2007GC001789.

Sun, D., R. Su, T. A. McConnaughey, and J. Bloemendal (2008), Variability of skeletal growth and $\delta^{13}C$ in massive corals from the South China Sea: Effects of photosynthesis, respiration and human activities, *Chem. Geol.*, *255*(3–4), 414–425, doi:10.1016/j.chemgeo.2008.07.012.

Swart, P. K. (1983), Carbon and oxygen isotope fractionation in scleractinian corals: A review, *Earth Sci. Rev.*, *19*(1), 51–80, doi:10.1016/0012-8252(83)90076-4.

Swart, P. K., R. E. Dodge, and H. J. Hudson (1996a), A 240-year stable oxygen and carbon isotopic record in a coral from South Florida: Implications for the prediction of precipitation in Southern Florida, *Palaios*, *11*(4), 362–375.

Swart, P. K., J. J. Leder, A. M. Szmant, and R. E. Dodge (1996b), The origin of variations in the isotopic record of scleractinian corals: II. Carbon, *Geochim. Cosmochim. Acta*, *60*(15), 2871–2885, doi:10.1016/0016-7037(96)00119-6.

Swart, P. K., G. F. Healy, R. E. Dodge, P. Kramer, J. H. Hudson, R. B. Halley, and M. B. Robblee (1996c), The stable oxygen and carbon isotopic record from a coral growing in Florida Bay: A 160 year record of climatic and anthropogenic influence, *Paleogeogr. Paleoclimatol. Paleoecol.*, *123*(1–4), 219–237, doi:10.1016/0031-0182(95)00078-X.

Swart, P. K., A. Szmant, J. W. Porter, R. E. Dodge, J. I. Tougas, and J. R. Southam (2005), The isotopic composition of respired carbon dioxide in scleractinian corals: Implications for cycling of organic carbon in corals, *Geochim. Cosmochim. Acta*, *69*(6), 1495–1509, doi:10.1016/j.gca.2004.09.004.

Swart, P. K., L. Greer, B. E. Rosenheim, C. S. Moses, A. J. Waite, A. Winter, R. E. Dodge, and K. Helmle (2010), The ^{13}C Suess effect in scleractinian corals mirror changes in the anthropogenic CO_2 inventory of the surface oceans, *Geophys. Res. Lett.*, *37*, L05604, doi:10.1029/2009GL041397.

Watanabe, T., A. Winter, T. Oba, R. Anzai, and H. Ishioroshi (2002), Evaluation of the fidelity of isotope records as an environmental proxy in the coral *Montastraea*, *Coral Reefs*, *21*(2), 169–178, doi:10.1007/s00338-002-0218-9.

Weber, J. N., P. Deines, P. H. Weber, and P. A. Baker (1976), Depth related changes in the $^{13}C/^{12}C$ ratio of skeletal carbonate deposited by the Caribbean reef-frame building coral Montastrea annularis: Further implications of a model for stable isotope fractionation by scleractinian corals, *Geochim. Cosmochim. Acta*, *40*, 31–39, doi:10.1016/0016-7037(76)90191-5.

Wei, G. J., M. Sun, X. H. Li, and B. F. Nie (2000), Mg/Ca, Sr/Ca and U/Ca ratios of a porites coral from Sanya Bay, Hainan Island, South China Sea and their relationships to sea surface temperature, *Paleogeogr. Paleoclimatol. Paleoecol.*, *162*(1–2), 59–74, doi:10.1016/S0031-0182(00)00105-X.

Wei, G. J., W. F. Deng, K. F. Yu, X. H. Li, W. D. Sun, and J. X. Zhao (2007), Sea surface temperature records in the Northern South China Sea from mid-Holocene coral Sr/Ca ratios, *Paleoceanography*, *22*, PA3206, doi:10.1029/2006PA001270.

Wei, G., J. Ma, Y. Liu, L. Xie, W. Lu, W. Deng, Z. Ren, T. Zeng, and Y. Yang (2013), Seasonal changes in the radiogenic and stable strontium isotopic composition of Xijiang River water: Implications for chemical weathering, *Chem. Geol.*, *343*, 67–75, doi:10.1016/j.chemgeo.2013.02.004.

Weil, S. M., R. W. Buddemeier, S. V. Smith, and P. M. Kroopnick (1981), The stable isotopic composition of coral skeletons: Control by environmental variables, *Geochim. Cosmochim. Acta*, *45*(7), 1147–1153, doi:10.1016/0016-7037(81)90138-1.

Yang, C., K. Telmer, and J. Veizer (1996), Chemical dynamics of the "St. Lawrence" riverine system: δD_{H2O}, $\delta^{18}O_{H2O}$, $\delta^{13}C_{DIC}$, $\delta^{34}S_{sulfate}$, and dissolved $^{87}Sr/^{86}Sr$, *Geochim. Cosmochim. Acta*, *60*(5), 851–866, doi:10.1016/0016-7037(95)00445-9.

Yu, K. F., T. S. Liu, T. G. Chen, J. L. Zhong, and H. T. Zhao (2002), High-resolution climate recorded in the $\delta^{13}C$ of *Porites lutea* from Nansha Islands of China, *Prog. Nat. Sci.*, *12*(4), 284–288.

Zhao, J. X., and K. F. Yu (2002), Timing of Holocene sea-level highstands by mass spectrometric U-series ages of a coral reef from Leizhou Peninsula, South China Sea, *Chin. Sci. Bull.*, *47*(4), 348–352, doi:10.1007/BF02901194.